# FLUIDIZATION OF ELECTRICALLY CONDUCTIVE PARTICLES IN AN ELECTRIC FORCE FIELD

M. K. Bologa and A. B. Berkov

UDC 541.182.3:537.212

Particle behavior is studied in an electrodynamically fluidized layer.

Electrodynamic fluidization of dispersed conductive and semiconductive materials [1] allows use of Coulomb forces to create a stable region of effective contact between solid and gaseous phases in the interelectrode gap and to perform intensive surface processing of the electrodes by the moving particles. For a number of practical applications such as heterogeneous catalysis and degasification of powders [1], deposition of coatings on electrodes and particles [1, 2], granulometric analysis [3], recording of ionizing radiation [4], and regulated heat removal and temperature stabilization [5, 6], use of electrodynamic fluidized beds is quite promising.

According to the concepts of [1, 3, 7] regarding motion of the dispersed component in a fluidized layer, all particles in the fluidization region move between the electrodes, recharging during collisions with the surface. The corresponding calculation model considers the representative oscillatory cycle of an isolated particle which upon contact with the electrode takes on a charge [8]

$$q_0 = \frac{\pi^3}{6}\varepsilon\varepsilon_0 d_T^2 E. \qquad (1)$$

The approximate nature of this model is related to neglect of the statistical character of particle motion, produced, in particular, by the presence of a quite wide spectrum of charge in the dispersed component in the fluidized region [9-11]. The goal of the present study is to develop an adequate physical picture of dispersed component motion in the electrodynamically fluidized layer.

The motion of the dispersed component of the layer was studied by stroboscopic photography in reflected light (strobe frequency $f = 5.33 \cdot 10^2$ Hz). The electrodynamic fluidization region 5 × 15 × 30 mm in volume was bounded by the copper electrodes of a planar horizontal capacitor with interelectrode gap h = 15 mm, optical windows spaced to accommodate the depth of field of the photographic equipment, 5 mm, and plastic inserts. A negative polarity high voltage U = 7.5-15 kV was applied to the upper electrode with the lower electrode being grounded. The dispersed component used was a powder of bronze spheres with density $\rho_t = 8.84 \cdot 10^3$ kg/m$^3$ and average size $\bar{d}_t = 286$ μm at mean volume concentrations $\bar{\beta} = 0.11$; 0.58; 1.67; 5.21%.

The photographs (Fig. 1) clearly show individual particle trajectories at mean volume concentrations $\bar{\beta} = 0.11\%$, and also at $\bar{\beta} > 0.11\%$ and field intensities $5 < \bar{E} \leq 6$ kV/cm (the threshold intensity for commencement of fluidization is equal to 5 kV/cm). The initial velocities and charges taken on by the particles after recoil from the electrodes are random quantities, which, in particular, is the cause of the significant number of discontinuous motions at the electrode surfaces (Fig. 1). At particle concentrations exceeding the critical value $\bar{\beta}_{cr}$ a precipitate layer is formed at the lower electrode, which is visible at $\bar{\beta} \geq 1.67\%$. Formation of the precipitate occurs due to reduction in field intensity at the lower electrode below the value for termination of electrodynamic fluidization under the action of the space charge of the moving particles.

Consideration of causes for the appearance of uncompensated particle charges in the fluidized region (homocharges, coinciding in sign with the sign of the nearer electrode, or heterocharges of opposite sign) leads to the following classification of volume electrification mechanisms in the electrodynamically fluidized layer. The inertial mechanism generates homocharges because of dispersion of colliding flows of oppositely charged particles; the recombination mechanism is caused by recombination of these flows; the gravitational mechanism is due

Applied Physics Institute, Academy of Sciences of the Moldavian SSR, Kishinev. Translated from Inzhenerno-Fizicheskii Zhurnal, Vol. 53, No. 1, pp. 77-84, July, 1987. Original article submitted April 15, 1986.

 0022-0841/87/5301-0802$12.50 

to the difference in velocities of flows upward and downward. The discontinuous particle motions are caused by formation of homo- or heterocharges depending on the sign of the particle and the height of their trajectories. Actual manifestation of the inertial and gravitational mechanisms of homopolar electrification is determined by the contributions of inertia and weight to the force balance of the moving particles.

With increase in concentration of the dispersed component the effect of space charge on the principles of electrodynamic fluidization increases. Accordingly, the particle mean volume concentration range can be divided into three regions: low ($0 < \bar{\beta} < \bar{\beta}_0$), moderate ($\bar{\beta}_0 \leq \bar{\beta} \leq \bar{\beta}_{cr}$), and stabilized ($\bar{\beta} > \bar{\beta}_{cr}$) concentrations of the dispersed component. At low concentrations the effect of particles on each other's motions is negligibly small. In the moderate concentration range accumulation of space charge changes the electric field in the interelectrode gap significantly. The upper concentration limit of this range $\bar{\beta}_{cr}$ corresponds basically to stabilization of the fluidized region field and commencement of formation of precipitates at the lower electrode. In the range $\bar{\beta} > \bar{\beta}_{cr}$ the dispersed component participates in electrodynamic fluidization with stabilized characteristics and a concentration corresponding to $\bar{\beta}_{cr}$ (the excess of particles forms a precipitate layer).

The stroboscopic photography produced quantitative information for cases in which individual particle trajectories were distinguishable. Transverse profiles of volume concentration and the mean absolute value of the particle velocity projection on the axis Oy, perpendicular to the electrode surface, were determined. Use of space–time averaging [12] with consideration of the multidispersity of the particles and replacement of integration over time by summation over intervals between stroboscope flashes for the set of images obtained gives the following dependence for processing of the original experimental data:

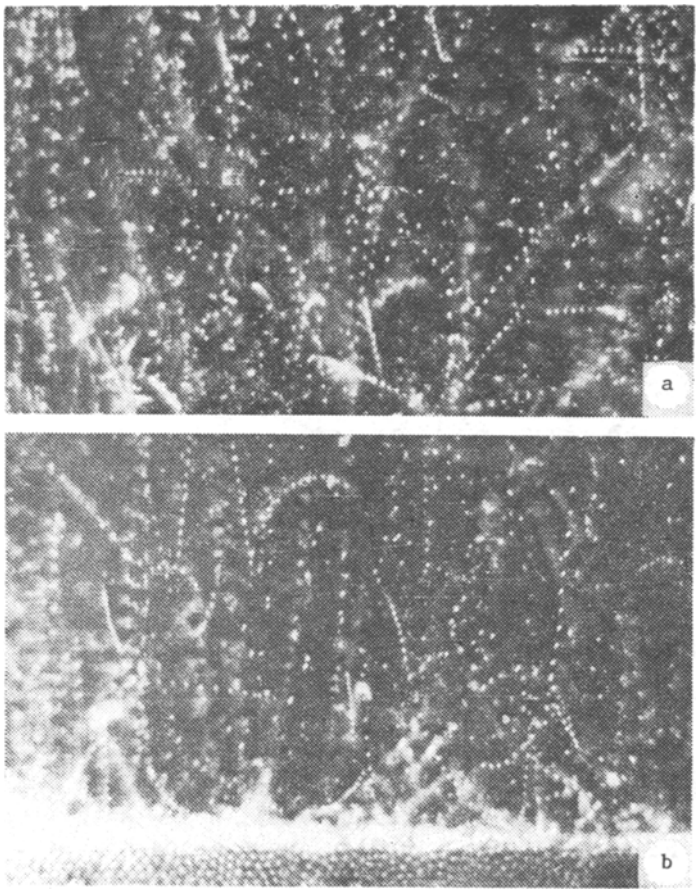


Fig. 1. Particle motion in stroboscopic illumination. a) $\bar{\beta}$ = 0.11%, $\bar{E}$ = 9 kV/cm; b) $\bar{\beta}$ = 5.21%, $\bar{E}$ = 7 kV/cm.

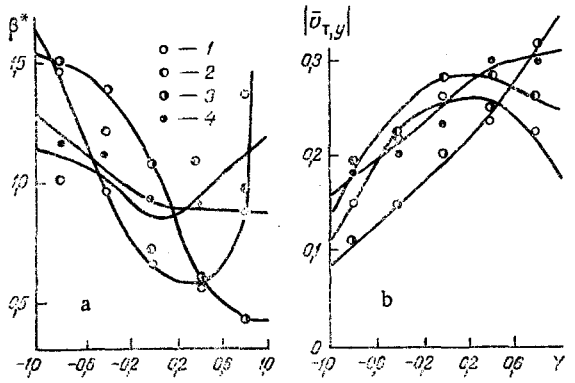


Fig. 2. Relative volume concentration $\beta^* = \beta/\bar{\beta}$ (a) and averaged transverse particle velocity $|\bar{v}_{t,y}|$ (b) distributions over section of horizontal planar capacitor (h = 1.5 cm, $\bar{E}$ = 6 kV/cm) vs volume concentration of dispersed component; 1-4) $\bar{\beta}$ = 0.11; 0.58; 1.67; 5.21%. $|\bar{v}_{t,y}|$, m/sec.

$$\beta = \frac{\int\limits_{\Delta t}\int\limits_{\Delta\Gamma} s\,d\Gamma\,d\tau}{\int\limits_{\Delta t}\int\limits_{\Delta\Gamma} d\Gamma\,d\tau} = \frac{\omega_\tau \sum\limits_{k=1}^{l} n_k}{l k_f \Delta\Gamma}, \tag{2}$$

$$|\bar{v}_{\tau,y}| = \frac{\int\limits_{\Delta t}\int\limits_{\Delta\Gamma} |v_{\tau,y}|\,s\,d\Gamma\,d\tau}{\int\limits_{\Delta t}\int\limits_{\Delta\Gamma} s\,d\Gamma\,d\tau} = \frac{\sum\limits_{k=1}^{l}\sum\limits_{i=1}^{n_k} |v_{\tau,y,k,i}|}{\sum\limits_{k=1}^{l} n_k}, \tag{3}$$

where $\Delta t$ and $\Delta\Gamma$ are the time and volume elements for the averaging, $\Delta t$ is the exposure time, equal to 1/30 sec; $\Delta\Gamma = 3 \times 5 \times 30$ mm is the band (height h = 3 mm), comprising 1/5 of the interelectrode distance, $\tau$, is the current time, s is an attribute of the dispersed medium, equal to 1 at points in space occupied by particles and to 0 at points occupied by gas, $n_k$ is the number of particle positions photographed in the k-th frame in $\Delta\Gamma$; $k_f$ is the number of stroboscope flashes per exposure; $l$ is the number of frames used in processing the data, $\omega_t$ is the particle volume. Local concentration and velocity distributions obtained by this method for $\bar{E}$ = 6 kV/cm are shown in Fig. 2.

Data were obtained for particle charging in the fluidized layer for the low dispersed component concentration range (in a homogeneous field in the interelectrode gap) for $\bar{\beta}$ = 0.11% and $\bar{E}$ = 6 and 8 kV/cm. To determine the charge of a particle moving along a trajectory recorded in a photographic frame the equation of motion

$$q = E^{-1}\left[ m\left( \frac{dv_{\tau,y}}{d\tau} + g \right) + F_{c,y}(|\mathbf{v}_\tau|)\,\mathrm{sign}\,(v_{\tau,y}) \right] \tag{4}$$

was used. Estimates made with the Ostrogradskii–Gauss equation indicate that homogeneity of the electric field is not distorted by the charges of moving particles by more than 1%.

The data obtained indicate that upon contact with an electrode the particle may not only incompletely recharge (change the sign of its charge after collision with the electrode by an amount significantly less than the charge determined by Eq. (1)), but may discharge slightly (maintain the sign of its charge after collision with the electrode). That is, the charge taken on by a particle in collision with an electrode is determined not only by the parameters of the medium surrounding the particle (field intensity, electrical conductivity of the contact interval separating the particle and electrode, etc.), but also by the particle charge before collision. The form of the particle distribution function over charge acquired in the steady state fluidization regime on the lower electrode surface is shown in Fig. 3 and corresponds qualitatively to the results of the experiments of [9] with micron particles of carbonyl iron, escaping from the fluidization region into a vacuum.

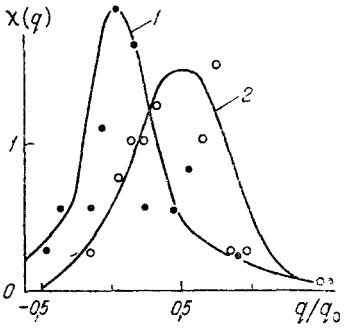


Fig. 3. Particle distribution over charge $\chi(q)$, acquired for steady state electrodynamic fluidization ($\bar{\beta}$ = 0.11%) on surface of lower electrode ($q_0$ is the contact charge of the particle calculated with Eq. (1)): 1) E = 8 kV/cm; 2) 6.

These features of charging of the dispersed component and acquisition of velocities of the particles after rebound from the electrode are the cause of the discontinuous or interelectrode character of their motion. With decrease in particle size the role of discontinuous motion in electrodynamic fluidization decreases, due to an increase in specific dissipation of kinetic energy caused by the viscous resistance force of the medium applied to the dispersed component. As a result, upon electrodynamic fluidization of micron particles their motion occurs along field force lines, while in individual cases, for example, for finely ground graphite powder, interelectrode motion of a "jet" of unipolarly charged particles occurs.

The critical mean volume concentration of the dispersed component and parameters of the precipitate layer formed on the lower electrode were determined by the local electrical conductivity method [13] using two fractions of graphite powder with mean dimensions $\bar{d}_t$ = 67 and 281 μm. Graphite was chosen as a material with low contact electrical resistance and satisfactory reproducibility of measurements. The electrodes were made of copper foil coated textolite. Two local electrical conductivity sensors were formed on the lower electrode (Fig. 4) with following geometric parameters: sensor interelectrode distance $l_{1,2}$ = 1 mm, $l_{2,3}$ = 3 mm, sensor electrode width d = 1 mm. The precipitate layer thickness was calculated from the interelectrode electrical resistance $R_{1,2}$, $R_{2,3}$ with consideration of a calibration function [13].

In the absence of a field, with the particle layer in a static state, the scattering of electrical resistances measured by the sensors did not exceed ±10%. When the local electrical conductivity method was used under electrodynamic fluidization conditions an increase was recorded in fluctuations of the interelectrode resistances $R_{1,2}$ and $R_{2,3}$, related to exchange of particles between the fluidized layer and the precipitate, as well as internal displacements or changes in orientation of particles in the precipitate layer. With increase in the thickness of the precipitate in the fluidized layer the internal structure of the former becomes more stable (the frequency and magnitude of sensor electrical resistances decrease, see Fig. 4). The increase in precipitate layer instability in the region $\bar{\beta} \to \bar{\beta}_{cr}$ is accompanied by a significant increase in sensor resistance $R_{1,2}$ and $R_{2,3}$ greater than 1 MΩ) and an increase in the sampled dispersion $\frac{1}{n}\sum_{i=1}^{n}(R_i-\bar{R})^2$ (where n is the number of measurements of resistance $R_i$), which under these conditions characterizes the frequency of formation of conductive "bridges" of individual particles between the sensor electrodes.

It was established by the local electrical conductivity method that for graphite particles of size $\bar{d}_t$ = 67 μm the quantity $\bar{\beta}_{cr}$ comprises 0.5-1%, while for $\bar{d}_t$ = 281 μm $\bar{\beta}_{cr}$ = 2-3%.

Determination of the quantity $\bar{\beta}_{cr}$ involves calculation of the capture radius $r_{ef}$, i.e., the maximum limiting distance at which charged particles collide under the action of interparticle electric forces. A simplified calculation of $r_{ef}$ was performed for a fluidized region model in the form of oppositely charged particle flows moving between the electrodes. A collision of two point charges of opposite sign ($q_1$, $q_2$) with identical mass m in the absence of external force fields will occur when their kinetic energy does not exceed the potential energy of interparticle interaction at a distance equal to the capture radius:

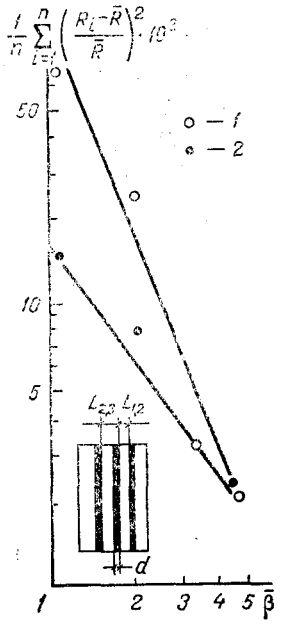


Fig. 4. Ratio of sampled dispersion to sampled mean indication of local electrical conductivity sensor vs mean volume concentration of graphite particles in fluidized region [$\bar{E}$ = 4 kV/cm; 1, 2) $\bar{d}_t$ = 281 and 67 μm] and fragment of sensors used. $\bar{\beta}$, %.

$$\frac{m}{2}(v_{\tau,1}^2 + v_{\tau,2}^2) = \frac{|q_1||q_2|}{4\pi\varepsilon\varepsilon_0 r_{ef}}. \tag{5}$$

According to results of calculations with Eq. (5) (with consideration of functions for determining the particle velocities $v_{t,1}$, $v_{t,2}$ by the method of [7]) for a copper dispersed component in the size range $d_t$ = 1-500 μm, fluidized in the homogeneous field of a planar capacitor with h = 1 cm, E = 7 kV/cm, the capture radius is 1-3 orders of magnitude less than the particle diameter. The effect of external electric and gravitational fields in the fluidized region decreases the value of $r_{ef}$. Thus, the particle capture radius in an electrodynamically fluidized region can be defined with consideration of the contact effect:

$$r_{ef} = d_\tau. \tag{6}$$

Using the latter relationship, we can estimate the number of particle collisions n during transit of the interelectrode gap (it is assumed that half the particles in the fluidized layer move upward, half, downward):

$$n = 3\bar{\beta}h/d_\tau. \tag{7}$$

For identical mean volume concentrations the probability of interparticle collisions is greater for larger particles under electrodynamic fluidization. For finely dispersed material, this fact together with the tendency to uniform interelectrode motion of micron particles leads to an increase in the role of the recombination mechanism of volume electrification.

The concept of a fluidized region at $\bar{\beta} = \bar{\beta}_{cr}$ in the form of a set of elementary cells (rectangular parallelepipeds of volume $d_t^2 h$ or regular hexagonal prisms of volume $[\sqrt{3}/2]\, d_t^2 h$), in which the individual particles move, allows definition of an expression for the possible range of $\bar{\beta}$ values:

$$\frac{\pi}{6}\frac{d_\tau}{h} \leqslant \bar{\beta}_{cr} \leqslant \frac{\pi}{3\sqrt{3}}\frac{d_\tau}{h}. \tag{8}$$

Estimates with Eq. (8) agree qualitatively with results of $\bar{\beta}_{cr}$ measurements performed by the local electrical conductivity method.

NOTATION

E, electric field intensity; $d_t$, m, q, diameter, mass, and charge of a particle; g, acceleration of gravity; h, interelectrode distance; Y, dimensionless transverse coordinate; $\beta$, local volume concentration of particles; $\varepsilon_0$, $\varepsilon$, dielectric permittivity of a vacuum, relative dielectric permittivity of gas; $\rho$, density of material. Subscripts: t, particle; y, projection of vector on Oy axis.

LITERATURE CITED


1. O. A. Myazdrikov, Electrodynamic Fluidization of Dispersed Systems [in Russian], Leningrad (1984).
2. S. A. Bolotin and S. V. Gegin, Elektron. Obrabot. Mater., No. 6, 17-19 (1979).
3. V. V. Romanenko, "Study of the electrogravitational principle of separation of powdered materials and processing methods and devices for control of dispersion composition," Author's Abstract of Candidate's Dissertation, Leningrad (1982).
4. O. A. Myazdrikov, V. N. Demidovich, and A. P. Suslov, At. Energ., 20, No. 5, 442-444 (1979).
5. Yu. E. Tetelya, V. V. Vishnevskii, V. P. Usenko, et al., Elektron. Obrabot. Mater., No. 4, 61-64 (1984).
6. A. B. Berkov, M. K. Bologa, V. V. Pushkov, and V. L. Solomyanchuk, Thermostabilization by Electrodynamic Fluidization of Dispersed Material [in Russian], Odessa (1985), Dep. NII-ÉIR, No. 3-7692.
7. M. K. Bologa, V. V. Pushkov, and A. B. Berkov, Izv. Akad. Nauk SSSR, Energ. Transp., No. 4, 109-116 (1980).
8. N. N. Lebedev and I. P. Skal'skaya, Zh. Tekh. Fiz., 32, No. 3, 375-378 (1962).
9. A. Y. H. Cho, J. Appl. Phys., 35, No. 9, 2561-2564 (1964).
10. V. I. Koryakov, V. A. Leonov, and D. N. Lezhnin, Elektron. Tekh., Ser. 10, No. 3, 12-22 (1967).
11. G. M. Colver, J. Appl. Phys., 47, No. 11, 4839-4849 (1976).
12. F. I. Frankl', Selected Works on Gas Dynamics [in Russian], Moscow (1973), pp. 669-687.
13. A. B. Berkov and F. E. Spokoinyi, The Possibility of Measuring Precipitate Layer Thickness by the Local Electrical Conductivity Method [in Russian], Minsk (1980), Dep. Informénergo, No. D/721.


# SOME SPECIAL FEATURES OF THE MASS TRANSFER OF THE LIQUID PHASE IN COMPOSITE MATERIALS BASED ON TUNGSTEN AND TITANIUM CARBIDES


A. F. Lisovskii and T. É. Gracheva



UDC 532.546:620.22



We investigated the phenomena of absorption of molten cobalt by the triphase composite (Ti, W)C–WC–Co and the moving forces of this process.


According to existing notions, mass transfer of metallic melts into sintered porous composites occurs under the effect of capillary forces [1, 2], and into nonporous ones under the effect of diffusion [3]. By the investigations of [4] it was proved that in sintered bodies consisting of high melting particles and a binder metal, a third kind of mass transfer is possible, viz., absorption of metallic melts by nonporous composite bodies induced by rearrangement of the high melting skeleton. This process was called migration of the liquid phase [5].

At present migration of the liquid phase is being investigated predominantly in biphase materials. Special features of the kinetics of mass transfer of metallic melts in triphase composites, the mechanism and the moving forces were not studied much.

The present work is intended to shed light on some of these regularities.

---


Institute of Superhard Materials, Academy of Sciences of the Ukrainian SSR, Kiev.


Translated from Inzhenerno-Fizicheskii Zhurnal, Vol. 53, No. 1, pp. 84-87, July, 1987. Original article submitted April 25, 1986.



0022-0841/87/5301-0807$12.50